JOURNAL OF MATERIALS SCIENCE **40** (2005) 2493–2498

Ceramic oxide bonds using calcium aluminosilicate glasses

L. ESPOSITO, A. BELLOSI
ISTEC-CNR, Via Granarolo 64, Faenza 48018, Italy
E-mail: laura@istec.cnr.it

Glasses with compositions falling in the Ca-Al-Si-O system are used to bond oxide ceramics. Alumina, zirconia and an alumina-zirconia composite are used as ceramic components. Joints are obtained at temperatures slightly higher than the melting temperature of glass which, for the selected compositions, change from 1210 to 1410°C. The degree of interaction between the ceramic components and the glass interlayer is mainly influenced by the bonding temperature and by the cooling rate. Conversely, the presence of defects like pores at the ceramic-glass interfaces depends on the experimental technique adopted to deposit the glass onto the ceramic surface. The 3-point flexural strength of the joint is measured at room temperature and for selected samples at 500°C. The mechanical properties of the joints are related to the microstructure at the interface.

1. Introduction

Alumina and zirconia and related composites have been widely investigated over the last several decades [1–4]. The characteristics of these oxides are mostly governed by the mean grain size and distribution, the composition and thickness of the intergranular phase and the compatibility and interactions among the involved components. The final microstructure depends on these features as well as on the degree of cation segregation (from impurities and/or sintering aids) that occurs during sintering and the consequent interfacial force balance arising between the grains [2].

The nature of the ceramic material and the interactions occurring at high temperature among the phases that come in contact are key to the degree of adhesion exhibited between two different materials [5–7]. In case of ceramic glass joints, the optimal glass composition is function of the ceramic material, in particular: (1) the glass must be chemically and thermo-mechanically compatible with the ceramic; (2) the glass must wet the ceramic; (3) the glass must melt below the temperature at which the ceramic starts to degrade; (4) the glass must have a relatively low viscosity in order to flow easily between the two ceramic parts.

The various phenomena occuring at the ceramic-glass interface at high temperature (elemental diffusion, partial penetration of glass, grain detaching and mobility, partial glass crystallization, etc.) can be accomodated to achieve reliable joints if the glass is properly selected. For instance, a sharp, weak ceramic-glass interface can be modified by grading the microstructure of the ceramic with the glass [8]. Alternatively, controlled devitrification of the glass interlayer can be employed to induce the formation of crystalline phases that can toughen the interfacial region [7].

In the following, calcium aluminosilicate glasses are tested as interlayers to bond three different ceramic materials: ZrO_2 stabilized with 3 mol% of Y_2O_3, a composite Al_2O_3-ZrO_2 and dense Al_2O_3. The microstructure and thermo-mechanical properties of the joints are presented and related to the phenomena occurring at high temperature among the involved materials.

2. Experimental

The compositions and principal characteristics of the ceramic materials and of the glasses are reported in Tables I and II, respectively. Dense ceramic samples obtained by sintering cylindrical pellets of ceramic powder that were linearly (100 MPa) and then cold isostatically pressed (150 MPa), were used in the experiments. The ceramic surfaces placed in contact during the bonding cycles were previously polished with diamond paste up to 15 μm.

The amount of glass needed to obtain an interlayer with the desired thickness was calculated using the surface area of the ceramic piece and the density of the glass. The glass powder (sieved below 25 μm) was deposited through a fine sieve (below 40 μm) onto

TABLE I Compositions, sintering conditions and some characteristics of the materials. α: thermal expansion coefficient (20–1200°C), σ: 4-pts R.T. flexural strength. $Z = ZrO_2$ Tosoh TZ-3YB containing 3 mol% of Y_2O_3. $A = Al_2O_3$ Alcoa CT3000. $AZ = 80Al_2O_3$-$20ZrO_2$ (wt%)

Material	Sint. Cycle (°C × h)	Density gr/cm^3(%)	α ($\cdot 10^{-6}$/K)	σ (MPa)
ZrO_2(Z)	1500 × 1	6.04 (99.8)	10	600 ± 20
Al_2O_3-ZrO_2(AZ)	1600 × 1	4.22 (98.4)	8.5	461 ± 15
Al_2O_3(A)	1600 × 1	3.95 (99.0)	8	349 ± 14

TABLE II Composition and properties of glasses. Density (ρ) measured with Archimede's method. Glass transition, softening and melting points measured with heating microscope analysis

	Composition wt% (mol%)							
Glass	SiO_2	Al_2O_3	CaO	$\alpha \cdot 10^{-6}$ (K^{-1})	ρ (g/cm^3)	G. Trans. (°C)	Soft. P. (°C)	Melt. P. (°C)
G1	34.0 (39.8)	39.8 (27.4)	26.2 (32.8)	6.62[a]	2.76	930	970	1400
G2	38.5 (43.3)	32.0 (21.2)	29.5 (35.5)	6.60[b]	2.76	900	950	1420
G3	61.8 (64.8)	14.9 (9.2)	23.3 (26.0)	5.50[c]	2.66	900	935	1210

[a]T. S. Tkachenko, R. Ya. Khodakovskaya, in Issledovaniya v Oblasti Khimicheskoi Technologii Proizvodstva Stekla I Stekloizdelii, Moskva, 1986, p. 90.
[b]Y. Hagasewa, Glastech Ber., 1984, Vol. 57, No. 7, p. 177; 1986, Vol. 59, No. 2, p. 53; 1986, Vol. 59, No. 7, p. 189.
[c]W. H. Dumbaugh, R. R. Genisson and M. R. Lestrat, US Patent No 3978362 Cl 2 H 01 K 1/28, 1/50 7/00, Off. Gazette, 1976.

TABLE III Processing conditions and results obtained on the tested samples. σ: 3-pts R.T. flexural strength

Sample #	Ceramic	Glass	Cycle I (°C × min)	Cycle II (°C × min)	Glass Calc. (μm)	Thickness final (μm)	σ (MPa)	$\sigma_{joint}/\sigma_{ceramic}$
1	Z	G1	1450 × 15	1450 × 20	25	0	77 ± 34	0.13
2	Z	G1	1450 × 10	1450 × 10	50	10–15	70 ± 11	0.12
3	Z	G2	1500 × 30	–	50	0	173 ± 88	0.29
4	Z	G2	1450 × 30	–	50	0	99 ± 56	0.16
5	Z	G3[a]	1250 × 10	–	50	50	56 ± 16	0.09
6	AZ	G1	1500 × 15	1500 × 10	50	40	224 ± 86	0.49
7	AZ	G1	1500 × 15	1450 × 10	50	40	250 ± 49[b]	0.54
8	AZ	G2	1450 × 30	–	50	40	191 ± 115	0.41
9	AZ	G2	1450 × 15	–	20	10	156 ± 82	0.34
10	A	G3	1250 × 10	1250 × 10	50	50	228 ± 53	0.65
11	A	G3	1250 × 10	1250 × 60	50	50	180 ± 33	0.52

[a]Glass was mixed with 10 vol% of cubic ZrO_2 powder (MEL SC 101).
[b]Strength measured at 500°C: 339 ± 57 MPa; at R.T. after an annealing cycle at 500°C, 146 ± 40 MPa.

the surface of one of the two halves of the sample. In some cases the surface of both halves was covered with half of the calculated glass amount. The glass amount deposited on the ceramic surface was controlled by weighing the sample during the sieving until the desired quantity was reached. With this technique more homogeneous glass powder layers were obtained compared to previous studies [8].

Bonding cycles were conducted in air in either a front loading or a bottom loading furnace. The bottom loading furnace could be opened at high temperature, allowing samples to be placed into or removed from the hot zone at the desired temperature. In this way it was possible to skip or reduce the heating and cooling steps, or assemble the two halves of a sample when the glass was still molten.

After bonding, the samples were cut and polished and the interfacial microstructure of the joints was analysed by optical microscopy (OM), scanning electron microscopy (SEM) and energy dispersive spectroscopy (EDS). The fracture strength of the bonds was evaluated at room temperature and at 500°C via 3-point bend testing on bars measuring 14.0 × 2.0 × 1.5 mm using a jig with 11 mm of span at a crosshead speed of 0.5 mm/min. Strengths were calculated using the standard formula.

3. Results and discussion

3.1. System ZrO_2—Calcium aluminosilicate glasses

Samples 1 and 2: Two different amounts of glass, equivalent to a thickness of 25 and 50 μm, respectively, were chosen for study (Table III). Each half of a given sample was covered with half of the calculated glass. The glass melted and coated the ceramic surfaces during the first heating cycle at 1450°C. After 10 min at this temperature the bottom part of the furnace was lowered and the two halves were assembled. The furnace was then closed and upon reaching 1450°C again, the second soaking step was begun. After the second cycle was completed, the samples were cooled in the furnace to 800°C at a cooling rate of 10°C/min and then the furnace was turned off. A faster cooling rate enhances the formation of cracks along the interface due to the thermal expansion mismatch between zirconia and glass (10 and 6.6 × 10^{-6}/K, respectively, Table I).

Samples 1 and 2 exhibited flexural strengths of 77 ± 34 and 70 ± 11 MPa, respectively. In all specimen fracture occurs along the ceramic-glass interface. The cross-sectional microstructure of these samples exhibits some pores and cracks at the interface (Fig. 1a). At the tested temperature and in presence of the selected glass, the attractive forces between the grains in the ZrO_2 decrease, leading to an intimate mix of ceramic grains and glass. This suggested that ideally the joint should be formed as a graded zirconia-glass microstructure in place of the original interface. Indeed, a graded microstructure could be formed but only in part of the overall interface (Fig. 1b). The presence of defects in the starting materials (pores, non homogenous density) led to some differences in the penetration rate of the glass and to pore formation in the compositionally graded microstructure. The poor mechanical resistance is likely due to the presence of these defects.

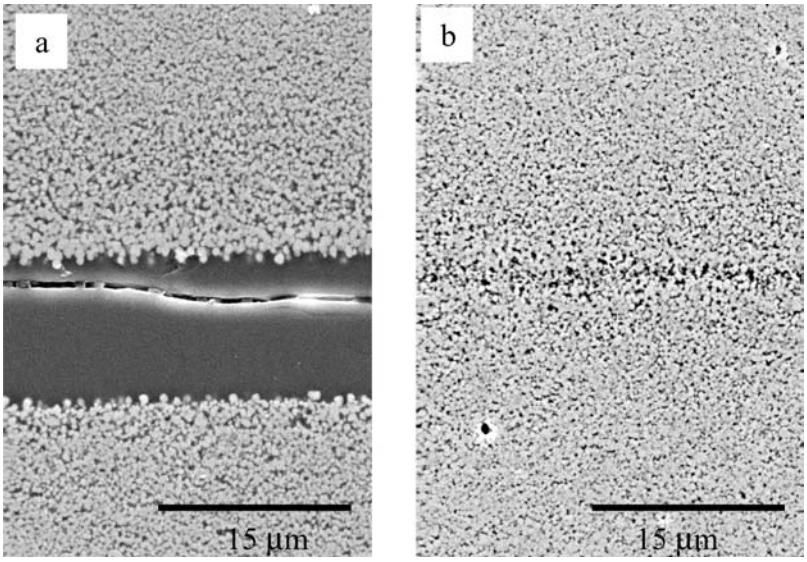

Figure 1 Cross-sectional microstructures of (a) Sample 1 and (b) Sample 2.

We found that the interrupted thermal cycle of the bottom loading furnace was suitable for the zirconia-silicate glass system. Zirconia exhibits a relatively high thermal expansion coefficient in comparison with the glasses. When zirconia is placed in contact with one of the glasses the expansion mismatch between the two materials promotes the formation of cracks along the interface, particularly in case of fast cooling rates. A bonding cycle characterised by slow heating and cooling steps would be better suited for this system.

Samples 3 and 4: These samples were joined in a single air-fired step using the front loading furnace, employing a slow heating and cooling rate. The heating cycles and mechanical properties are presented in Table III and the final glass thickness in Fig. 2.

The glass penetrated into zirconia during the bonding cycle leading to a microstructure similar to those described for Samples 1 and 2. In case of Samples 3 and 4 however, the glass did not crack because the rate of cooling after joining was much slower. The extent of the glass penetration is function of the initial amount of glass, the bonding temperature and the soaking time, as shown in the plot of Fig. 2. The interface is characterized by a homogeneous distribution of quasi-spherical zirconia grains and glass phase, similar to the microstructure of Sample 2 presented in Fig. 1b. The ZrO_2 particles have a grain size comparable to the as-sintered material (0.7–1 μm) but with a more spherical shape due to the dominating repulsive forces between the particles when these are immersed in the molten glass [9]. The two ceramic pieces appear to be so intimately joined that in some regions the position of the original interface can be found only by using a residual pore as a marker. As in the case of the previous samples, the penetration front of the glass depends on the defects in the ceramic substrate. Consequently, pores caused by glass decomposition or degassing phenomena coexist with regions containing a thin residual glass layer. From the mechanical point of view this lack of microstructural homogeneity leads to a large scattering of the flexural strength values (173 ± 88 and 99 ± 56 MPa for samples 3 and 4, respectively).

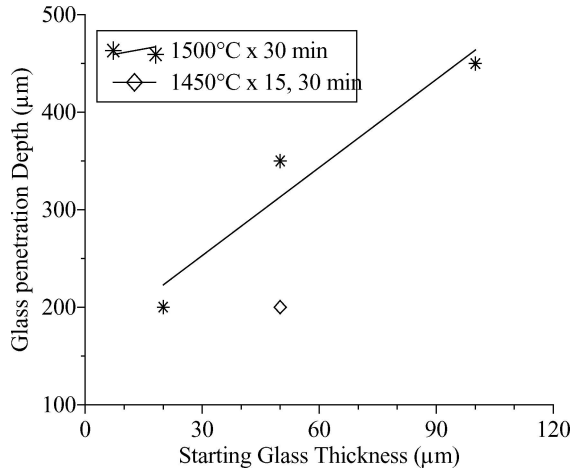

Figure 2 Penetration depth of glass in ZrO_2–based ceramic in function of the starting G2 glass interlayer thickness. The results presented elsewhere are also reported [8].

Sample 5: The previous four samples demonstrated that the use of calcium aluminosilicate glasses that melt at a temperature of 1400°C or higher, which is only 100°C lower than the sintering temperature of zirconia, promotes a rapid but poorly controlled penetration of the glass within the grain boundaries of the ceramic. This penetration leads not only to the expected formation of a graded structure in place of the weak ceramic-glass interfaces, but also to pores and to regions with thin layers of glass. The mutual mobility between the zirconia particles and these glasses is energetically favored under the experimental conditions adopted for this sample, and can be hardly controlled by changing the heating parameters (heating and cooling rate, soaking time, etc.). With this ceramic/glass combination, therefore, it is extremely difficult to promote the formation of a uniform, pore-free joint.

As an alternative, a glass with a lower melting temperature was selected in order to decrease the joining temperature up to a value at which little or no

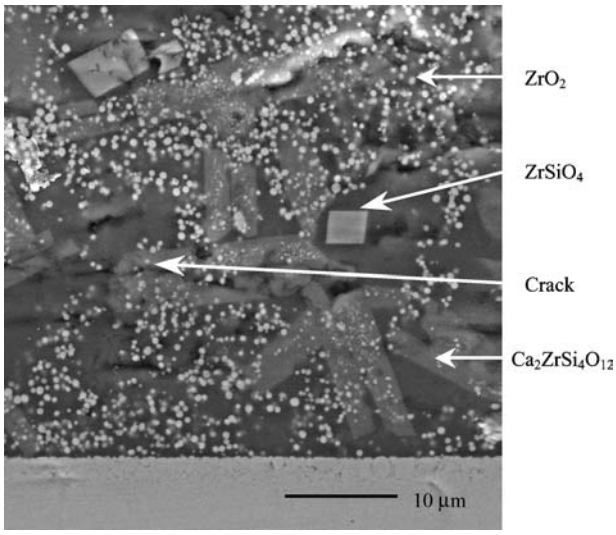

Figure 3 Ceramic-glass interface of Sample 5.

penetration of glass within the grain boundaries of the ceramic would occur. Glass G3 has a melting point approximately 200°C lower than those of glass as G1 and G2 but exhibits a larger thermal expansion mismatch with ZrO_2. If used alone, it would be expected to readily crack upon cooling. In order to avoid this problem, in Sample 5 a small amount of ZrO_2 powder was mixed with the glass prior to the deposition onto the ceramic surface (Table III). Using this mixture as the bonding agent led to the formation of a microstructure similar to those observed in previous samples, but with the difference that the ZrO_2 particles were lightly aggregated and not homogeneously mixed with glass as seen in Fig. 3. In addition, crystallization occurred during cooling, leading to the formation of elongated crystals of $Ca_2ZrSi_4O_{12}$ and squared crystals of $ZrSiO_4$. Under these conditions cracks formed within the glass interlayer, one of which is shown in Fig. 3. Consequently, the flexural strength of this sample was low (Table III).

3.2. System Al_2O_3-ZrO_2 (80–20wt%) —Calcium aluminosilicate glasses

Samples 6 and 7: These two samples were bonded at 1500°C in the bottom loading furnace following the same procedure described for Samples 1 and 2. In Sample 6 the glass powder (equal to a thickness of 50 μm) was deposited onto one of the two halves whereas in Sample 7, the powder was spread equally onto both halves. This slight difference in processing conditions was observed to have little effect on the final properties of these samples. Of the two, Sample 7 exhibits the best flexural strength and lower scatter 250 ± 49 MPa (Table III) a value which is 54% of the bulk ceramic. The flexural strength value of this sample increases significantly at 500°C (339 ± 57 MPa, Table III). The strength increase is probably due to the decrease, at 500°C, of the thermal expansion mismatch between the ceramic and the glass, and of the residual stresses that arise during the sample machining operations. Sample 7 was re-tested at room temperature after an annealing cycle at 500°C. In this case the flexural strength decreased (146 ± 40 MPa) probably because the stresses due to the thermal expansion mismatch were high again.

The cross-sectional microstructures of Samples 6 and 7 each reveal a uniform joint region containing partially devitrified glass of about 50 μm, no evidence of cracking and very few bubbles of 20 μm or less in diameter (Fig. 4). Devitrification led to the formation of elongated anorthite crystals. Clusters and chains of small, spherical grains of ZrO_2, which is partially soluble in this glass, also grew with a dendritic shape mainly at the edges of the anorthite grains. Zirconia is a nucleating agent for crystallization in glasses [10], and the small crystals which precipitated in the glass during the cooling step promoted the crystallization of anorthite. Conversely, no alumina dissolved within the glass. The selective zirconia dissolution led to the formation at the ceramic-glass interfaces of an alumina layer where the glass filled the holes left by dissolved zirconia. The similarities in microstructure and strength observed

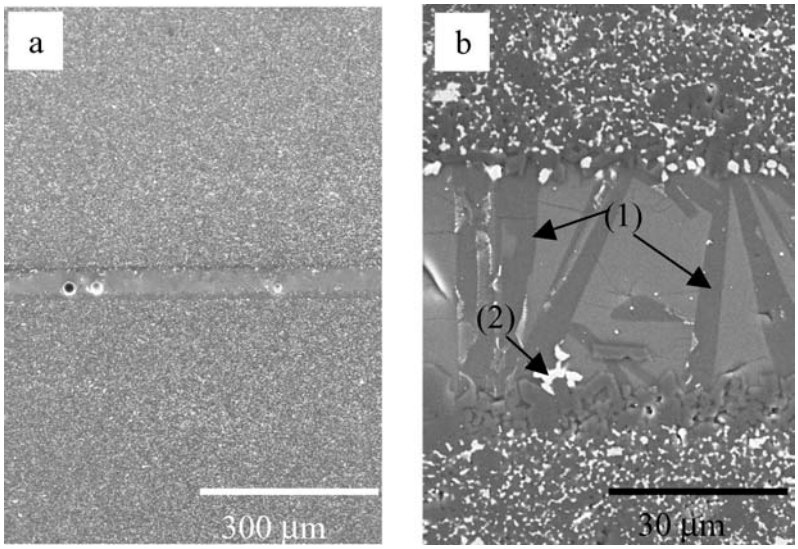

Figure 4 Cross-sectional microstructures of (a) Sample 6 and (b) Sample 7. The arrows indicate crystals of (1) elongated anorthite $CaO{\cdot}Al_2O_3{\cdot}2SiO_2$ and (2) dendritic zirconia.

between Samples 6 and 7 indicate that neither the temperature of the second soaking step nor the glass deposition methodology affects the final integrity of the joint. In addition, the use of a bottom loading furnace allows to shorten the bonding cycle with no deleterious effect on the quality of the joint.

Samples 8 and 9: These samples were air processed using the front loading muffle furnace and employing a single step heat treatment cycle. The glass powder (G2, Table II) was deposited in equal amounts on both substrate halves (Table III). The glass did not penetrate into the ceramic although both surfaces in contact with the glass were slightly depleted in zirconia. As with the previous samples, the glass wet the ceramic extensively, flowing along the surfaces and forming either a glassy or partially crystallized interlayer. Large needles of anorthite, $CaO{\cdot}Al_2O_3{\cdot}2SiO_2$, formed as determined by EDX analysis and confirmed by X-ray diffractometry performed on the fracture surfaces of the bend bar specimens. These anorthite appeared to grow perpendicular to the interface. The formation of this phase is in agreement with the original composition of the glass, which falls in the primary phase field of this phase in the ternary diagram SiO_2-Al_2O_3-CaO [11].

Samples 8 and 9 exhibit a lower value of flexural strength and a larger degree scattering in the date in comparison to Samples 6 and 7. This is due to the presence of pores in the glass interlayer that formed during the bonding cycle. Even though Samples 8 and 9 were heat treated at 1450°C, it is likely that viscosity of this high melting point glass is still too high to afford complete closure of pores along the interface. In addition these samples were bonded in only one cycle, which likely promoted the formation of pores of entrapped air within the glass interlayer.

3.3. System Al_2O_3—Calcium aluminosilicate glass

Samples 10 and 11: These samples were bonded using G3 as the glass interlayer and processed in the bottom loading furnace. Two cycles were adopted, the first to homogeneously coat with the glass one half of the sample, the second to produce the bond.

In the case of Sample 10 the furnace was switched off after the high temperature soak step and the temperature fell rapidly to 600°C in a few minutes. In Sample 11 a cooling rate of 300°C/h and of 200°C/h for the first and second cycle, respectively, was adopted.

Samples 10 and 11 were bonded at lower temperature compared to samples where G2 or G1 were used since G3 melts at about 1200°C. At this temperature, no interdiffusion and/or dissolution-precipitation phenomena were observed. The interfaces between the glass and the ceramic are quite clean, with the difference of a slight devitrification in the case of Sample 11, which is characteristic of the slower cooling rate (Fig. 5).

The flexural strength values are similar to those of the composite Samples 6 and 7 (Table III), but the interfaces are straight and the glass interlayers show little to no crystallization. Relative to the flexural strength of the ceramic material the strength of these joints are the highest of all those tested. In addition, Sample 11 exhibits the lowest amount of scattering of all the tested samples. We suspect that the use of two bonding cycles inhibits the pore formation at the interface, thus increasing the reliability of the joint.

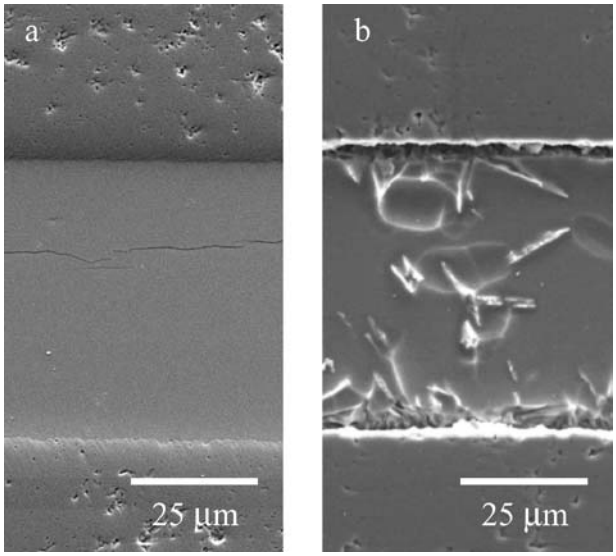

Figure 5 Microstructure of (a) Sample 10 and (b) Sample 11.

4. Conclusions

The bonding process and consequent adhesion between two ceramic parts by means of a glass interlayer is affected by the nature of the ceramic materials. Alumina and zirconia-based materials interact differently when in contact at high temperature with the same silicate glasses. Within the temperature range investigated in the present paper (1250–1500°C) dense zirconia forms graded structures where the ceramic grains and the glass are intimately mixed together. Alumina on the contrary forms almost straight interfaces with partially crystallized glass interlayers. Alumina-zirconia composites form bonds with a partially crystallized interlayer enriched with reprecipitated zirconia crystals.

In all the three systems bonds can be obtained, but their reliability is strongly function of the experimental procedure. In particular, in case of zirconia, the control of the interdiffusion between the ceramic grains and the glass is critical for inhibiting the pore formation or, conversely, the cracking of the residual glass at the interface. The best results were obtained with a single heating cycle at 1500°C (173 ± 88 MPa). The best results for the alumina-zirconia composite (250 ± 49 MPa) and the alumina (228 ± 53 MPa) were obtained with two heating cycles: the first is to coat homogeneously the ceramic surface with the glass, the second to form the bond with the other ceramic part.

Acknowledgements

The authors wish to thank Cesare Melandri for the mechanical testing.

References

1. R. BRYDSON, S.-C. CHEN, F. L. RILEY, S. J. MILNE, X. PAN and M. RÜHLE, *J. Am. Ceram. Soc.* **81**(2) (1998) 369.
2. N. RAVISHANCAR and C. B. CARTER, *Acta Mater.* **49** (2001) 1963.
3. NETTLESHIP, B. P. PATTERSON and W. S. SLAUGHTER, *J. Am. Ceram. Soc.* **86**(2) (2003) 252.
4. O. VASYLKIV, Y. SAKKA and V. V. SKOROKHOD, *ibid.* **86**(2) (2003) 299.
5. L. ESPOSITO, A. BELLOSI and S. LANDI, *ibid.* **82**(12) (1999) 3597.
6. A. P. TOMSIA, A. M. GLAESER and J. S. MOJA, *Key Eng. Mat.* **111/112**, (1995) 191.
7. W. A. ZDANIEWSKI, P. M. SHAH and H. P. KIRCHNER, *Adv. Ceram. Mater.* **2**(3A) (1987) 204.
8. L. ESPOSITO and A. BELLOSI, *Scripta Mat.* **45** (2001) 759.
9. H.-H. PARK, S.-J. L. KANG and D. N. YOON, *Metall. Trans. A* **17** (1986) 325.
10. G. H. BEALL and D. A. DUKE, "Glass Science and Technology," edited by D. R. Uhlmann and N. J. Kreidl (Academic Press, New York, 1983), Vol. I, p. 403.
11. E. M. LEVIN, C. R. ROBBINS and H. F. MCMURDIE, "Phase Diagrams for Ceramists" (American Ceramic Society Inc., Columbus Ohio, 1964), Fig. 630, p. 219.

Received 31 March
and accepted 18 July 2004